UNIVERSITY OF CALIFORNIA,
IRVINE

Analysis of Flood Conditions in Mekong Delta in Vietnam,
Based on Sentinel Data

THESIS

submitted in partial satisfaction of the requirements
for the degree of

MASTER OF SCIENCE

in Civil and Environmental Engineering

by

Chufan Feng

Thesis Committee:
Assistant Adjunct Professor Phu Dinh Nguyen, Chair
Professor Kuolin Hsu
Assistant Professor Tirtha Banerjee

2021

TABLE OF CONTENTS

LIST OF FIGURES iii
LIST OF TABLES..... iv
ACKNOWLEDGEMENTS v
ABSTRACT OF THE THESIS vi
INTRODUCTION 1
CHAPTER 1: Previous Literatures and Content of the Paper 2
CHAPTER 2: Study Area and Data Source 6
CHAPTER 3: Methodology 9
CHAPTER 4: Results and Discussion 14
CHAPTER 5: Conclusion 24
REFERENCE 26

LIST OF FIGURES

Figure 1. Location of Mekong River Basin and Mekong Delta 7
Figure 2. Comparison of Surface Water Maps based on Sentinel-1 Data 14
Figure 3. Comparison of Surface Water Maps based on Sentinel-2 Data 15
Figure 4. Comparison of Surface Water Maps in More Detail 16
Figure 5. One-to-one Version of True Map and Selected Map 17
Figure 6. Frequency Map from 2016 to 2020 18
Figure 7. Permanent Water Map from 2016 to 2020 19
Figure 8. Trend of Total Surface Water from 2016 to 2020 20
Figure 9. Trend of Seasonal Surface Water from 2016 to 2020 20
Figure 10. The Inundated Pixels in Extreme Events from 2016 to 2020 22
Figure 11. The Affected Area Trend in Extreme Events from 2016 to 2020 22
Figure 12. The Exposed Population in Extreme Events from 2016 to 2020 23
Figure 13. The Exposed Population Trend in Extreme Events from 2016 to 2020 23

LIST OF TABLES

Table 1. Thresholds for Different Polarization Modes 10
Table 2. Thresholds for Different Water Indices 11
Table 3. Rules of Dividing the Permanent or Non-permanent Water....................................13
Table 4. Accuracy for Image in Oct. 2019 (High Cloud Cover)..15
Table 5. Accuracy for Image in Feb. 2019 (Low Cloud Cover)...16
Table 6. Annual Maximum Events Selection from 2016 to 2020 21
Table 7. Affected Area in Extreme Events from 2016 to 2020..22
Table 8. Exposed Population in Extreme Events from 2016 to 2020....................................23

ACKNOWLEDGEMENTS

I would like to express the deepest appreciation to Professor Phu Dinh Nguyen, who agreed to be my thesis advisor immediately, during this pandemic time. In-time e-mail responds all the time, more encouragement than pressure, and timely reminders and proper requirements… Professor Phu not only brings me useful advice in research, but also cares about my mental and living conditions, which impressed me a lot. Without his guidance and persistent help this thesis would not have been possible.

I would also like to thank Professor Kuolin Hsu and Professor Tirtha Banerjee, for agreeing to be my committee members, which allows me to get great confidence and encouragement when I first started my research. In addition, I would like to say thank you to Angie Zuniga, the Graduate Coordinator in Department of Civil and Environmental Engineering. Thanks for helping me with my confusions when I write and prepare to submit the thesis paper.

Finally, thanks Han Gao – my roommate for comforting me during my hardest time. Also, thanks Jamboree – my cat for waiting and accompanying me at every night. All experiences are precious and unforgettable to me.

ABSTRACT OF THE THESIS

Analysis of Flood Conditions in Mekong Delta in Vietnam,

Based on Sentinel Data

by

Chufan Feng

Master of Science in Civil and Environmental Engineering

University of California, Irvine, 2021

Assistant Adjunct Professor Phu Dinh Nguyen, Chair

Mekong river is a trans-boundary river in east Asia and southeast Asia, flows through six countries: China, Myanmar, Laos, Thailand, Cambodia, and Vietnam. Due to the abundant water resources and diverse biological resources, the Mekong River Basin has been always significant. However, there have been natural problems in the Mekong River Basin for a long time, such as the extreme droughts in the Upper Basin and floods in the Lower Basin, especially in Mekong Delta in Vietnam. Through literature review, there are few studies on flood conditions in the Mekong Delta in recent years, and it is particular rare to find researches applying the Sentinel Data. Therefore, in this paper, Sentinel-1 SAR and Sentinel-2 MSI Imageries are used to conduct the analysis of flood conditions in Mekong Delta, based on the Google Earth Engine (GEE) Platform.

In the first part of this study, different surface water extraction methods are assessed. The Single-band Threshold Method is used for Sentinel-1 SAR data, and the surface water is extracted based on two different polarization modes ("VV" and "VH"). At the same time, Multi-Band Threshold Method is used for Sentinel-2 MSI data, and surface water is extracted based on different water indices, considering NDWI, MNDWI, LSWI, AWEI and WI indices. After analyzing the accuracy of different methods, the Sentinel-1 data with the "VV" polarization mode performs

the best, with the Overall Accuracy of 0.8618 and 0.9204 in two scenarios. In the second part, all data can be processed to extract the water surface through 2016 to 2020, using the Sentinel-1 data with the “VV” polarization mode. Then, the permanent water and non-permanent water can be classified. More specifically, the pixels that recognized as water with a frequency greater than 0.7 are classified as the permanent water. Accordingly, under the time series, the trends of total surface water and the seasonal surface water can be generated. In the final part, a simple damage assessment is conducted, to compare the annual extreme flood events. As a result, in the past five years from 2016 to 2020, the most extreme flood event occurred in 2018, with the affected area of 695,117 hectares and the exposed population of 1,500,517.

INTRODUCTION

The Mekong River is known as the twelfth longest river in the world and the sixth longest river in Asia (Liu et al., 2009). It is an important trans-boundary river that flows through six countries in East and Southeast Asia, including China, Myanmar, Laos, Thailand, Cambodia, and Vietnam. The Mekong River generally flows from northwest to southeast, and empties into the sea from the Mekong Delta in the southwestern Vietnam. The Mekong Basin spans large parts of continental Southeast Asia, which is endowed with rich natural resources, and has been always important for people's survival and social-economic development in the basin area (Leinenkugel et al., 2015). Since the twenty-first century, climate change is an environmental problem faced by human beings all over the world. One of the major dangers is the sea level rise. Due to the low-lying terrain, the Mekong Delta region is facing the risks of flooding caused by rising sea level (*Report*, n.d.). In addition to the sea level rise, high tides, dykes and land subsidiarity (VietnamPlus, 2019) are also the causes of increasingly serious floods in cities in the Mekong Delta. Since its important position and great risks, it is necessary to study the water resources, especially the flood analysis, in the Mekong Delta region.

In 2000, an exceptionally severe flood event occurred in Mekong Delta. Since then, there have been studies focusing on flood monitoring and flood hazard forecasting. The research of flood is often inseparable from the extraction of surface water. In order to obtain images with shorter return period and higher resolution, so as to improve the accuracy of surface water extraction and then get more reasonable analysis and prediction, researchers are paying more and more attention to Sentinel Data, which is an Earth observation mission from the Copernicus Programme developed by European Space Agency (ESA) (*Missions - Sentinel Online - Sentinel*, n.d.). Among them, the most commonly used Sentinel-1 mission provides Radar imaging that regardless of the weather conditions. Besides, the Sentinel-2 mission provides high-resolution optical imagery that allows to monitoring objectives such us vegetation, soil, and coastal areas (*Missions - Sentinel*

Online - Sentinel, n.d.). In general, Sentinel Data is suitable for flood analysis and surface water extraction in Mekong Delta region.

The overall objective of this study is to investigate the current situation of flood in Mekong Delta, selecting a relatively accurate method to extract the surface water in the study area, especially the seasonal flood water surface, and then conduct a trend and disaster analysis. The study is based on the Google Earth Engine (GEE) platform so as to process all acceptable data, and provides ideas for further flood mitigating methods and managements.

CHAPTER 1: Previous Literatures and Content of the Paper

1.1. Review of Flood Research in Mekong River Basin

The Mekong River Basin covers an area of 795,000km^2 (Commission (MRC), n.d.), spanning 26 degrees of latitude, and embracing various ecosystems. It is a representative research area for various methodologies and remote sensing application research fields (Arias, 2013). However, in fact, the number of studies on the Mekong River Basin is not as high as imagined. One possible reason can be, the Mekong River Basin is covered by continuous clouds for most of the year, so that it is difficult to obtain high-quality remote sensing data of similar time phases in the whole area, especially in Upper Mekong Basin (Cvar, 2013).

Since the extreme flood event in 2000, the flood-related research has gradually increased, which indicates people's greater attention to this field. Reiner W. et al. (2004) assessed the impact of sea level rise in Mekong Delta and delineated the areas with different levels of vulnerability (Wassmann et al., 2004). Toshihiro Sakamoto et al. (2007) detected the temporal changes in the extent of annual flooding within the Mekong Delta based on MODIS time series imagery (Sakamoto et al., 2007). Dinh Q. et al. (2012) analyzed flood hazard, vulnerability and risk with the major focus on Long Xuyen Quadrangle which is the most important region in the Mekong Delta (Dinh et al., 2012). In the same year, Boateng, I (2012) assessed the vulnerability to climate change with the major focus on coastal area (Boateng, 2012).

Recent years, researchers began to use different remote sensing imagery to explore the flooding situation in Mekong Delta. Felix Greifeneder et al (2013) conducted the flood detection and inundation mapping using synthetic aperture radar (SAR) imagery, and proved for its usability (Greifeneder et al., 2014). Claudia Kuenzer et al (2015) analyzed the inundation patterns and characteristics of four Asian river deltas including Mekong Delta in time series, based on MODIS Reflectance data (Kuenzer et al., 2015). In 2017, Binh Duc Pham et al developed a methodology to detect and monitor surface water and conduct the flood mapping using Sentinel-1 SAR data.

It is worth mentioning that, the destruction of cropland is one of the largest impacts of floods in the Mekong Delta. Therefore, there are plenty of research also attaching great importance to the impact of flood events on cropland when studying flood events or flood frequencies (Wassmann et al., 2004) (Wassmann et al., 2019) (Hoang-Phi et al., 2020).

1.2. Overview of Water Extraction Methods

Surface water is one of the most important sources of people's domestic water and agricultural irrigation in the Mekong River basin, and it is also an indispensable support for the development of fishing industry in the lower Mekong River (Sneddon & Fox, 2006). At present, there are two main methods for surface water extraction. One is the extraction based on machine learning algorithm, which is an object-oriented classification method for remote sensing images. The most commonly used are the Random Forest (RF) algorithm, Support Vector Machine (SVM) algorithm, and Neural Network (NN) algorithm.

The other one is the extraction based on spectral features of remote sensing images, including Single-band Threshold Method and Multi-band Threshold Method. At the beginning, researchers tended to use the Single-band method to distinguish water bodies, but sometimes the ground objects that absorbing a certain band will seriously affect the classification accuracy (Zhou et al., 2019). For Multi-band Method, the application of water index has developed rapidly and is widely used. In recent twenty years, many water indices have been put forward and improved. Mcfeeters (1996) proposed NDWI (Normalized Difference Water Index), which allows the water body to be enhanced and the vegetation information to be effectively suppressed. Xu (2005) modified NDWI on this basis, and the proposed MNDWI (Modified Normalized Difference Water Index) that can reveal more subtle features of water body. K. Chandrasekar (2010) established LSWI (Land Surface Water Index) that is sensitive to the liquid water in vegetation and the corresponding soil background. Feyisa (2014) developed the index AWEI (Automatic Water Extraction Index), making the extraction of water body more accurate in special environment in the world. For example, in images with large area of shadows or black soils. Danaher (2006) created WI_{2006} (Water Index) based on Landsat-7 ETM+ imagery, and Fisher (2016) improved WI_{2015} to extract water or wetland information.

1.3. Current Applications of Sentinel Data

Sentinel-1 SAR mission allows observations that regardless of the weather conditions, day and night, and has a comparable spatial resolution to visible and near-infrared satellite images (Brisco et al., 2008). Accordingly, it has become an important source of research regarding flood detection or surface monitoring. Galya B. (2018) conducted the segmentation of inland water surface in Great Hungarian Plain (Gálya et al., 2018). Kenduiywo (2018) mapped the crop-types through the growing seasons (Kenduiywo et al., 2018). Sentinel-1 SAR data can be also used to detect glacier and snow cover (Andreassen et al., 2019).

Sentinel-2 MSI mission obtains the Optical images of the earth surface with the spatial resolution of 10 -60 meters (Drusch et al., 2012), which is a high-quality remote sensing data that can be obtained stably. Moreover, there are large parts of the research tend to study the synergic use of

Sentinel-1 and Sentinel-2 images, to conduct the soil moisture mapping (El Hajj et al., 2017) (Das et al., 2019), the groundwater potential zones mapping (Nigussie et al., 2019), and detection of crops (Poenaru et al., 2018) or wildfires (Brown et al., 2018).

1.4. Overview of Google Earth Engine (GEE) Platform

Satellites monitor the surface of earth, and transmit the acquired data back to ground satellites. These images with high spatial and temporal resolution need to be processed by professional image processing software, such as ENVI and SNAP (Sentinel Application Platform that specific software for Sentinel Data processing) (*SNAP – STEP*, n.d.). However, due to the limitations of local computer performance, more and more researchers began to use Google Earth Engine (GEE) cloud computing platform to process these complex data.

Google Earth Engine (GEE) is a cloud computing platform that enables global researchers to acquire and process massive remote sensing images without huge workload. In general, GEE provides the technical support for resources and environment monitoring in global dimension. In field of surface water, Pekel J.F. and Cottam A. (2016) studied the high-resolution mapping of long-term changes of global surface water and quantified the changes in the past 32 years. Research on extracting and monitoring surface water based on water index is often carried out on GEE, especially the ones focusing on specific river basins or lakes in the world (Zou et al., 2018) (Xia et al., 2019).

There are types of research conducted on GEE platform. Besides surface water-related research, many researchers pay attention to snow cover assessment (Wayand et al., 2018), spatial distribution of forest (Shao et al., 2020), and cropland classifying and monitoring (Mirelva & Nagasawa, 2019).

1.5. Contents of Study

This study analyzes the flood conditions and extreme events in recent five years (2016-2020) in

Mekong Delta, based on the Google Earth Engine platform and Sentinel Data. More specifically, in the first part of the study, Both Sentinel-1 SAR and Sentinel-2 MSI Data are used to extract the surface water area in Vietnam Mekong Delta, applying the Thresholding Method. Two polarization modes in Sentinel-1 SAR and five water indices computed in Sentinel-2 MSI Data are considered, and the resulting maps are compared to the true maps that extracted from Landsat Data. As the results, the most accurate and reasonable extracting method is obtained for further flood analysis.

The second part applies the best water extraction method and threshold value to all the data from 2016 to 2020, and determines the permanent water and non-permanent water surface in the study area according to the frequency. Moreover, the trends of surface water are obtained, and also qualitatively compared with trends of permanent and non-permanent water surface.

The third part of the study focuses on the specific extreme events. The annual largest flood events can be selected through the previous results, and then used to conduct a simple damage analysis. The exposed population and affected area can be shown and computed, when comparing the surface water maps before and during the events.

CHAPTER 2: Study Area and Data Source

2.1. Overview of Mekong Delta

Mekong river is a trans-boundary river in east Asia and southeast Asia, with an estimated length of 4,350 kilometers. It flows from the Tibetan Plateau in China and runs through 6 countries. Mekong River basin in the southeast Asia, brought together these 6 countries – China (specifically Yunnan Province), Myanmar, Laos, Thailand, Cambodia and Vietnam. The Mekong River Basin is always divided into three parts, the Upper Mekong Basin, the Middle Mekong Basin, and the Lower Mekong Basin. The study area in this research is the Mekong Delta that located in the

Lower Mekong Basin in Vietnam. Due to the plain dominated terrain and the livable natural environment, the Mekong Delta has dense population, rich species and sound ecological system, and has been known as “Biological treasure trove” (Fantz, 2021). However, low coastal terrain makes it vulnerable to climate change and it is easy to cause environmental problems (*Report*, n.d.).

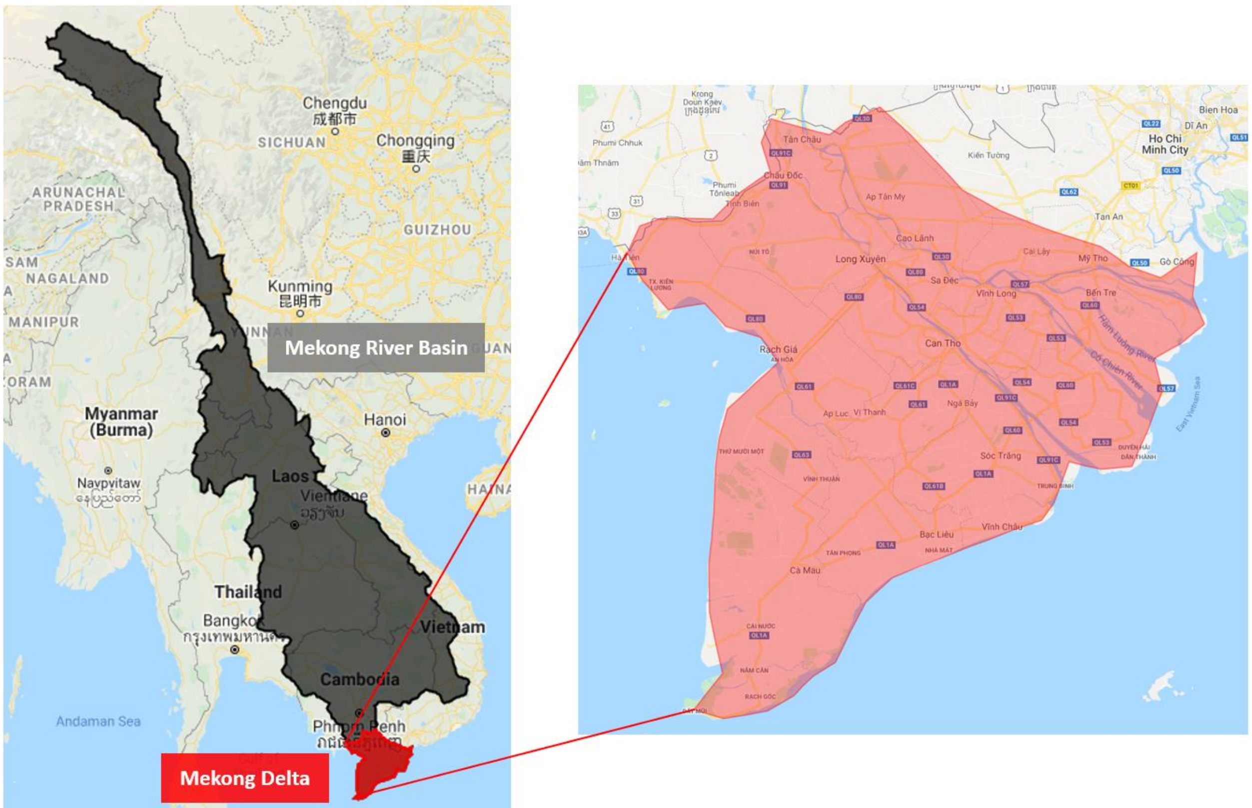

Figure 1. Location of Mekong River Basin and Mekong Delta

In 2000, there was a once-in-70-year catastrophic flood event in Mekong Delta. About 800 people lost their lives due to the extreme flood event, and the economic damage was over 400 million dollars (Weichselgartner, 2004). Also, in 2011, this area experienced another severe flood event that resulted in an estimated economic loss of 600 million dollars (*MEKONG FLOODS ARE A REMINDER OF A PERENNIAL RISK*, n.d.). From 2000, Mekong River Commission (MRC) has made a lot of efforts to reduce and control flood hazards. For example, the Flood Management and Mitigation (FMM) Strategy was developed, in order to monitor and forecasting the river flood (Commission (MRC), n.d.).

2.2. Data Source

In this study, Sentinel-1 SAR and Sentinel-2 MSI data are both considered to extract the surface water in the study area. For Sentinel-1 SAR data, the simple Single-band Threshold Method is applied, based on two polarization modes (VV and VH). For Sentinel-2 MSI data, the Multi-band Threshold Method is applied to calculate different water indices and then extract water surface. The reason for considering both data types is that Sentinel-1 and Sentinel-2 have their own advantages. The multi-band data provided by Sentinel-2 is convenient to calculate and improve different water indices, but it is greatly affected by clouds, while the radar data provided by Sentinel-1 can be unaffected by weather and clouds. For the study area which is cloudy all year round, considering two data types is helpful to get more accurate results (*Missions - Sentinel Online - Sentinel*, n.d.).

2.2.1. Sentinel-1 SAR Data and Pre-processing

Sentinel-1 mission provides data from a dual-polarization C-band Synthetic Aperture Radar (SAR) instrument, and contains the Ground Range Detected (GRD) scenes. It has four imaging modes: Strip Map Mode, Interferometric Wide Swath (IW), extra-wide Swath Mode (*Sentinel-1 SAR GRD: C-Band Synthetic Aperture Radar Ground Range Detected, Log Scaling*, n.d.). In this study, the IW Mode is selected. The Sentinel-1 Datasets in GEE has been pre-processed by the thermal noise removal, radiometric calibration, terrain correction and log scaling. Therefore, the only thing that need to be done is to filter the speckles, which allows to reduce the inherent speckle-effect of radar images (*Step-by-Step*, n.d.).

2.2.2. Sentinel-2 MSI Data and Pre-processing

Sentinel-2 is a multi-spectral, high-resolution and wide-swath mission, providing 13 bands with 3 different spatial resolution (*Sentinel-2 MSI*, n.d.). The Sentinel-2 data that applied in this study is Level-2A imagery, which has been pre-processed by atmospheric correction. In order to obtain images without impact on high cloud cover, the cloud removal need to be further done for Sentinel-2 L2A data (*Sentinel-2 MSI*, n.d.).

2.2.3. Other Built-in Datasets in Google Earth Engine

There are lots of built-in datasets that can be applied easily. JRC (Joint Research Centre) Monthly Water History Layers is a monthly average surface water layer that extracted based on Landsat 5, 7, and 8 images (Pekel et al., 2016), which is used and regarded as the true water maps in this study. This dataset is used to assess and select the best water extraction method, by calculating the overall accuracy of the confusion matrix.

GHSL Global Human Settlement Layers is also mentioned in this study, when briefly assessing the damage and exposed population of annual maximum flood event. This dataset contains the information of population density (*Global Human Settlement - GHS BUILT-UP GRID - European Commission*, n.d.), so that it can provide a more specific figure for us to understand the annual maximum flood.

CHAPTER 3: Methodology

3.1. Water Extraction for Sentinel-1 SAR Data

The Single-band Threshold Method is used to conduct the water extraction for Sentinel-1 SAR Data. The Sentinel-1 Data provides two polarization modes, which are “VV” and “VH”. Under the selected IW imaging method, the water surface shows darker than the land surface. In this case, if the appropriate threshold is found, the water surface and land can be simply classified. Regarding the determination of threshold, firstly, a suitable value is confirmed as the initial value from the histogram of pixel values. The threshold can be adjusted and improved, after verifying the corresponding accuracy and interpreting visually. The initial values and improved values of threshold are shown in the following table.

Table 1. Thresholds for Different Polarization Modes

Polarization Modes	Initial Threshold	Improved Threshold
VV	-16.0	-12.0
VH	-19.0	-19.7

Using the above improved threshold values to classify the image. On GEE platform, the first step is to add a new layer. Next is to add the value "1" to pixels that are above the threshold, as it represents water surface. Then add the value "0" to pixels below the threshold, as it represents non-water surface. Therefore, the water and non-water surface can be displayed based on this layer. Also, it works to only display water pixels by masking off the non-water pixels. Moreover, the expected resulting maps are two surface water maps based on different polarization modes of Sentinel-1 Data.

3.2. Water Extraction for Sentinel-2 MSI Data

The Multi-band Threshold Method is used to conduct the water extraction for Sentinel-2 MSI Data. The Sentinel-2 Data has 13 bands with 3 different spatial resolution. Therefore, it is feasible to calculate various water indices and apply them directly to the surface water extraction. In the literature review, a lot of water indices have been continuously improved for many years, and different indices are suitable for different situations. In this study, five water indices are selected, which are NDWI (Mcfeeters, 1996), MNDWI (Xu, 2005), LSWI (Chandrasekar et al., 2010), AWEI (Feyisa et al., 2014), and WI (Danaher & Collett, 2006) (Fisher et al., 2016). The formula that applicable to bands of Sentinel-2 Data can be summarized as follows.

$$NDWI = \frac{GREEN - NIR}{GREEN + NIR} = \frac{B3 - B8}{B3 + B8}$$

$$MNDWI = \frac{GREEN - SWIR}{GREEN + SWIR} = \frac{B3 - B11}{B3 + B11}$$

$$LSWI = \frac{NIR - SWIR}{NIR + SWIR} = \frac{B8 - B11}{B8 + B11}$$

$$AWEI = BLUE + 2.5GREEN - 1.5(NIR + SWIR1) - 0.25SWIR2$$

$$= \mathrm{B2} + 2.5\ \mathrm{B3} - 1.5\ (\mathrm{B8} + \mathrm{B11}) - 0.25\ \mathrm{B12}$$

$$WI_{2015} = 1.7204 + 171GREEN + 3RED - 70NIR - 45SWIR1 - 71SWIR2$$

$$= 1.7204 + 171\ \mathrm{B3} + 3\ \mathrm{B4} - 70\ \mathrm{B8} - 45\ \mathrm{B11} - 71\ \mathrm{B12}$$

After computing all the indices and adding them to the bands of the images, the image is ready to be classified, using the Threshold Method which is similar to the previous Single-band Threshold Method.

The initial threshold value of all five indices is zero (Wang D Z et al., 2019). The improvement of the thresholds is the same as previously mentioned. The initial values and improved values of threshold are shown in the following table.

Table 2. Thresholds for Different Water Indices

Different Water Index	Initial Threshold	Improved Threshold
NDWI	0	0.03
MNDWI	0	0.35
LSWI	0	0.42
AWEI	0	0.12
WI	0	7.30

The water pixels and non-water pixels can be chosen to display, if applying the improved thresholds. There are five expected resulting maps that based on different water indices computed in Sentinel-2 Data.

3.3. Accuracy Analysis

This process aims to compute the accuracy of all seven surface water maps that generated from

Sentinel-1 and Sentinel-2 Data. The true map is determined as the JRC Monthly Water History Layer which is the build-in dataset based on Landsat Imagery. In addition, the Overall Accuracy (OA) and Kappa Coefficient are selected as the index of accuracy verification.

The specific realization process of the accuracy analysis in GEE is based on pixel level. Generally, pixels with different attribute values can be counted when using the "Reduce" function (*Reducer Overview | Google Earth Engine*, n.d.). Therefore, it works for us to count for the number of pixels that are ① all “0”, ② all “1”, ③ tested to be “0” but in fact “1”, and ④ tested to be “1” but in fact “0”. Accordingly, the confusion matrix can be obtained, and then the Overall Accuracy and Kappa Coefficient can be computed. The above process can be realized by coding in GEE.

In order to compare the accuracy of different resulting maps more reasonably and sufficiently, in this process, the assessment is conducted under cloudy and cloudless conditions. By comparing the Overall Accuracy and Kappa Coefficient, as well as their stability, a more suitable dataset and water surface extraction index are selected.

3.4. Permanent Water Classification

Previous steps have chosen the best method to distinguish water surface from non-water surface. This step is to distinguish permanent water from non-permanent water (or seasonal water) according to frequency. According to the previous papers and considering the feasibility, the permanent water and non-permanent water are divided based on the frequency of the pixels that has been inundated.

More Specifically, the first step is to extract the water surface, applying the determined method and threshold on all eligible data in the past five years from 2016 to 2020. Secondly, the frequency of the inundated pixels can be calculated as the times that the pixel has been recognized as water dividing by the total recognition times, shown as equation (*). Then, we define that when a pixel has a frequency greater than 0.7 that has been identified as water, it is a permanent water surface;

and if the frequency identified as water is less than 0.7, then this pixel is seasonal water surface. To make it clearer, the rules of dividing the permanent or non-permanent water are shown in the following table.

$$Frequency = \frac{times\ of\ the\ pixel\ is\ inundated\ (be\ recognized\ as\ water)}{times\ of\ the\ pixel\ is\ recognized} \qquad eq(*)$$

Table 3. Rules of Dividing the Permanent or Non-permanent Water

Frequency > 0.7	Permanent Water Surface
Frequency < 0.7	Non-permanent Water Surface

According to this rule, the permanent water in the study area can be displayed. In addition, when masking off the permanent water, the seasonal water and trends can be shown.

3.5. Brief Damage Assessment

After the above steps, the trend of seasonal water surface under the time series can be obtained. Accordingly, the annual maximum flood event can be determined based on the total number of inundated pixels. In the damage assessment, the flooding area and exposed population in the annual maximum flood event in the past five years has been calculated and analyzed.

The calculation of flood area is straightforward. The inundated pixels can be counted, so the difference layer can be obtained when we mask off the water pixels before the flood in the image during the flood. In other words, difference layer shows the difference between before-flood image and during-flood image. Then, through the conversion of units, the flood area in this event can be calculated. Moreover, if the layer of population density is applied, it can be intersected with the difference layer. Therefore, the exposed population can be displayed and calculated.

CHAPTER 4: Results and Discussion

4.1. Comparison of Water Extraction Results

4.1.1. Spatial Comparison of Water Surface Maps

For consistency, I used the surface water extraction map in October 2019 as a display. The surface water maps generated from Sentinel-1 and Sentinel-2 images can be obtained and shown as follows. In the maps, the white area is non-water surface while the blue area indicates water surface. The true map is also shown for spatial comparison. It should be mentioned that due to the orbit limitation of Sentinel-1 Data, the information for the delta range is incomplete. However, this will not affect the flood information and accuracy test of most parts of delta.

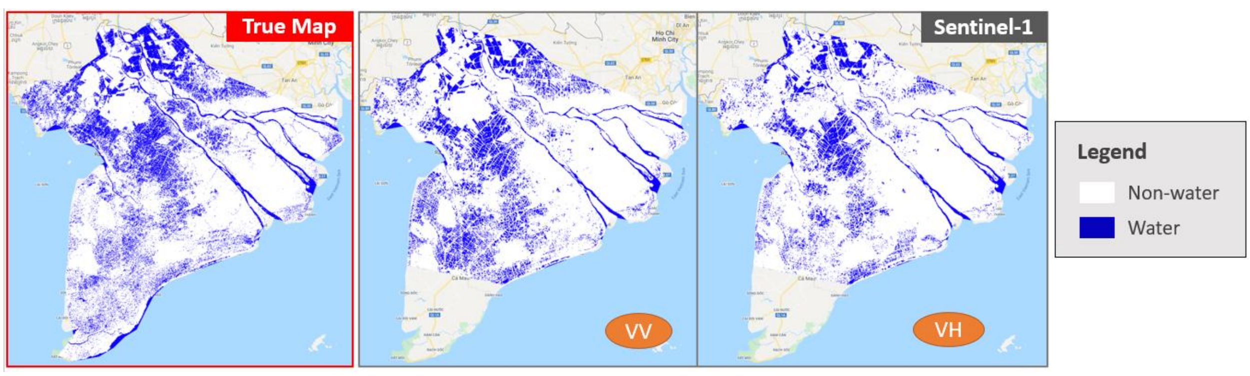

Figure 2. Comparison of Surface Water Maps based on Sentinel-1 Data

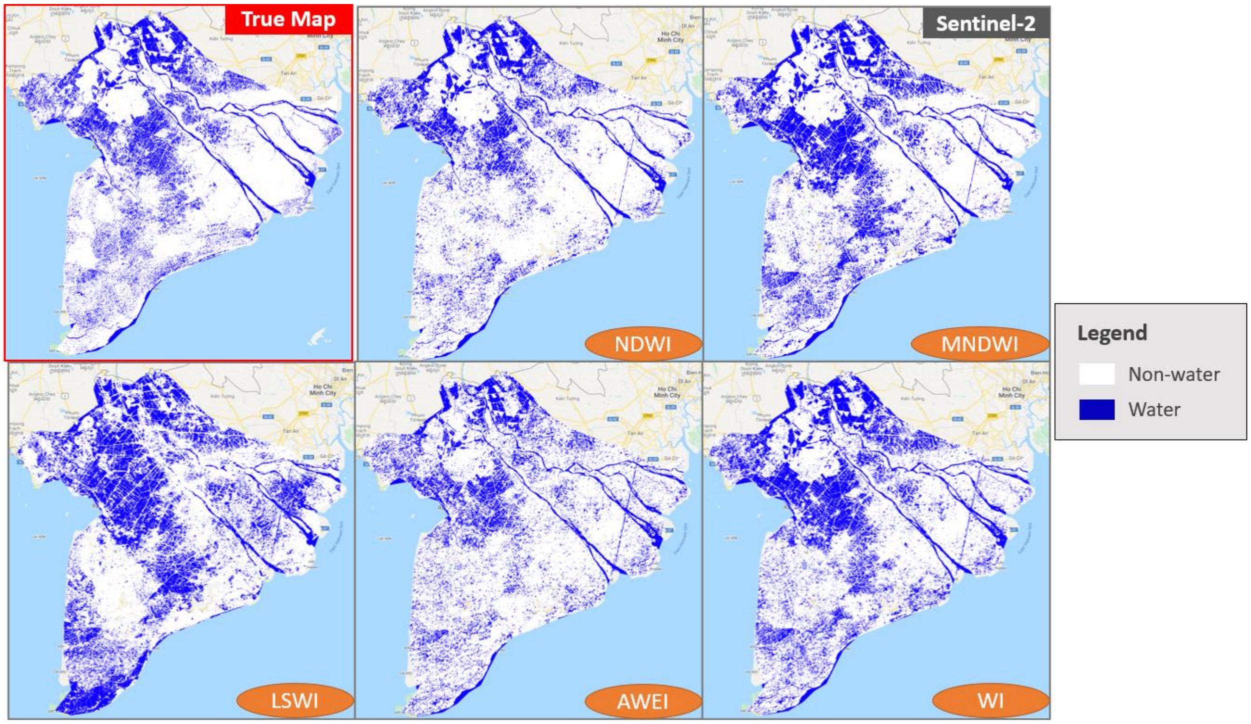

Figure 3. Comparison of Surface Water Maps based on Sentinel-2 Data

It is difficult to assess which map is closest to the true map only by naked eye observation, so it is necessary to consider accuracy calculation while visually observing.

4.1.2. Accuracy Analysis and Comparison

Applying the determined thresholds, the accuracy of surface water classification can be evaluated based on the true map. The accuracy for images in October 2019 and February 2019 is computed.

Table 4. Accuracy for Image in Oct. 2019 (High Cloud Cover)

Datasets	Polarization/ Index	Thresholds	Overall Accuracy	Kappa Coefficient
Sentinel-1 SAR	VV	-12.00	0.8618	0.5767
	VH	-19.70	0.8650	0.5952
Sentinel-2 MSI	NDWI	0.03	0.8827	0.6582
	MNDWI	0.35	0.8639	0.6207
	LSWI	0.42	0.7632	0.3745
	AWEI	0.12	0.8296	0.5405
	WI	7.30	0.8502	0.5902

Table 5. Accuracy for Image in Feb. 2019 (Low Cloud Cover)

Datasets	Polarization/ Index	Thresholds	Overall Accuracy	Kappa Coefficient
Sentinel-1 SAR	VV	-12.00	0.9204	0.5252
	VH	-19.70	0.9296	0.5877
Sentinel-2 MSI	NDWI	0.03	0.9162	0.5629
	MNDWI	0.35	0.9054	0.4570
	LSWI	0.42	0.7539	0.0093
	AWEI	0.12	0.8702	0.3936
	WI	7.30	0.8977	0.4507

From the above tables, the first four lines show better accuracy, which are surface water maps based on VV, VH, NDWI and MNDWI.

4.1.3. Selecting the Best Resulting Map

Combined with the results of accuracy assessment, we can compare maps with better accuracy in more detail. In the following figure, the small red squares indicate the obvious difference between the surface water map and the true map.

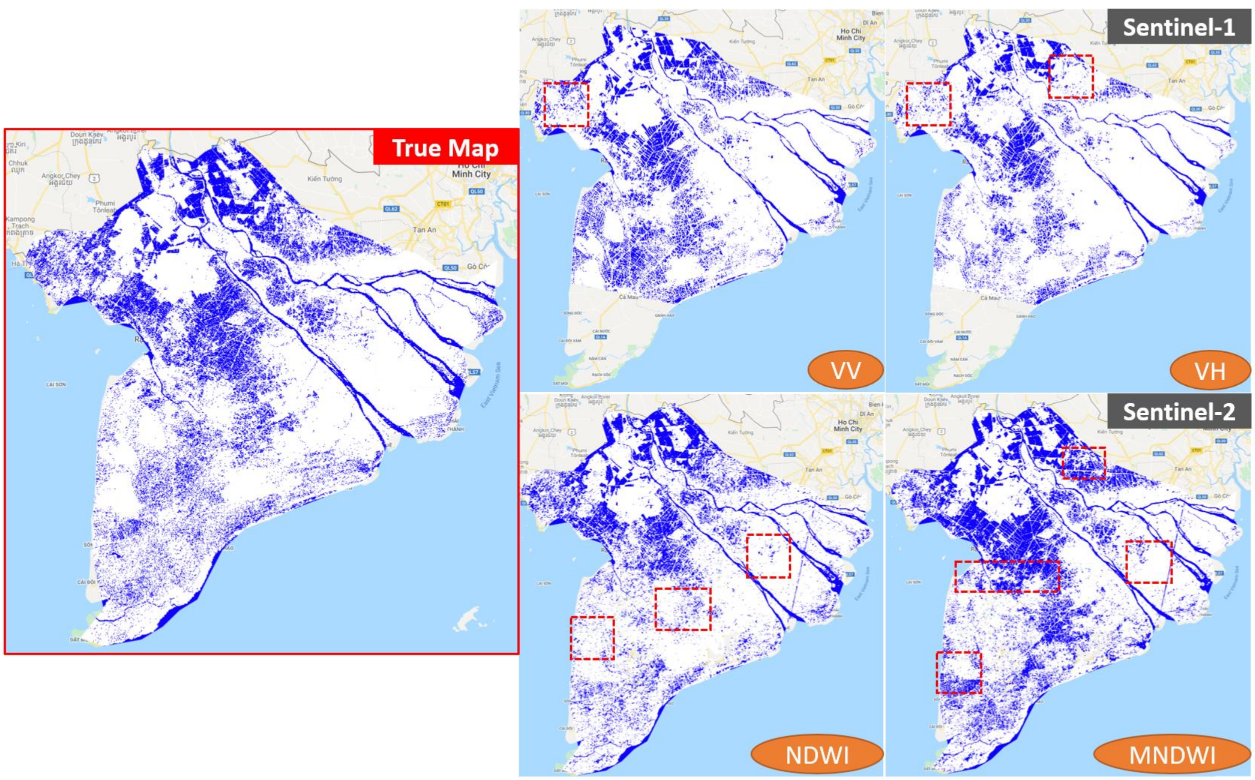

Figure 4. Comparison of Surface Water Maps in More Detail

It can be easily seen that water extraction from Sentinel-2 Data has more speckles or noises, so the boundaries of the surface water bodies are not clear. By comparison, the Sentinel-1 Data enables water bodies to have more clear-cut boundaries. Comparing the two polarization methods, “VV” polarization provides more stable results when changing the threshold values.

As a result, the Sentinel-1 SAR Data and its “VV” polarization mode are selected for further analysis. The one-to-one version of the true map and the selected map shows in the following figure.

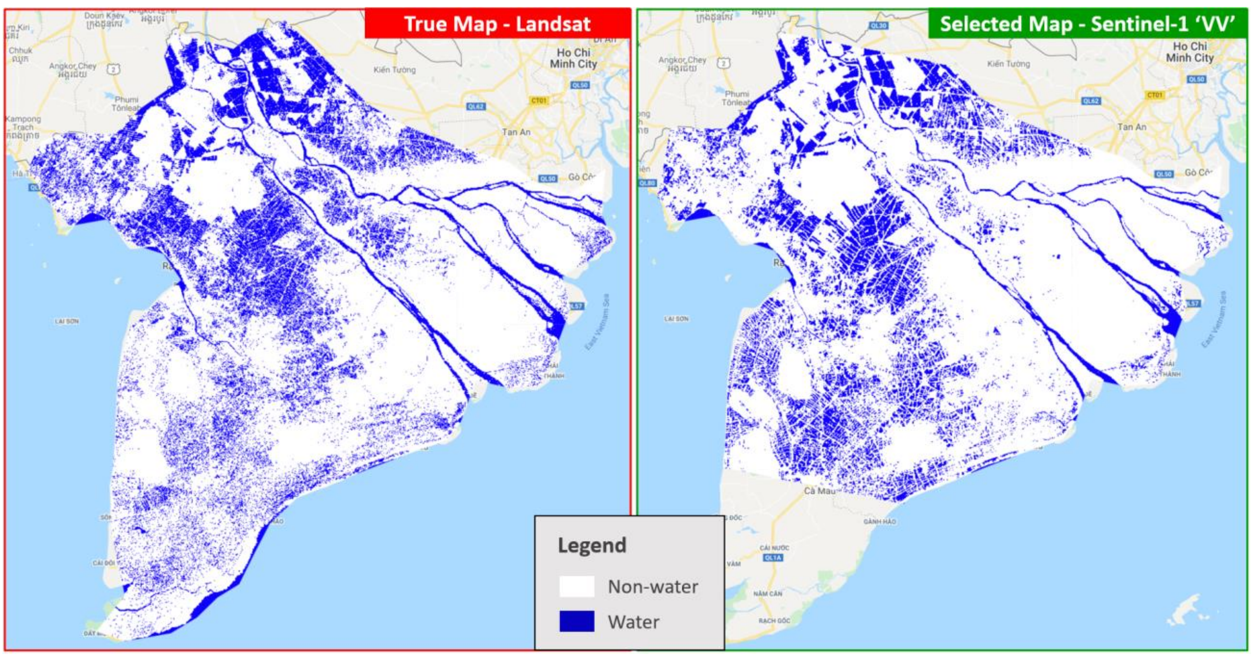

Figure 5. One-to-one Version of True Map and Selected Map

4.2. Permanent Water and Seasonal Water

4.2.1. Determining the Permanent Water

The water surface is extracted from all the acceptable data in the past five years from January 1st 2016 to December 31st 2020, and there are 273 scenes of data that met the requirements and had a unified range.

For the results, the frequency map is generated as follows, when the bright color represents high frequency of water surface, and the dark color represents low frequency of water surface.

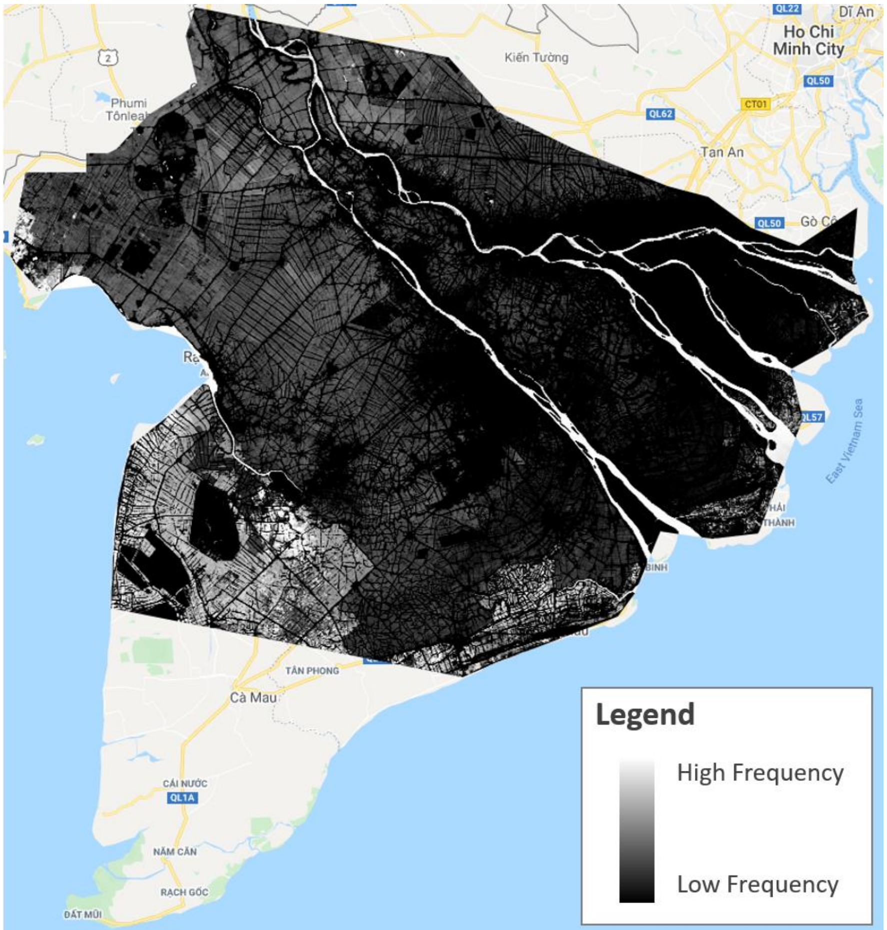

Figure 6. Frequency Map from 2016 to 2020

The frequency of 0.7 is used as the threshold to distinguish the permanent water surface, and then the permanent and the non-permanent water surface can be displayed. In this permanent water surface map, we can clearly see the boundaries of Mekong River and some small tributaries. Also, the rivers near the estuary are richer in water than inland areas.

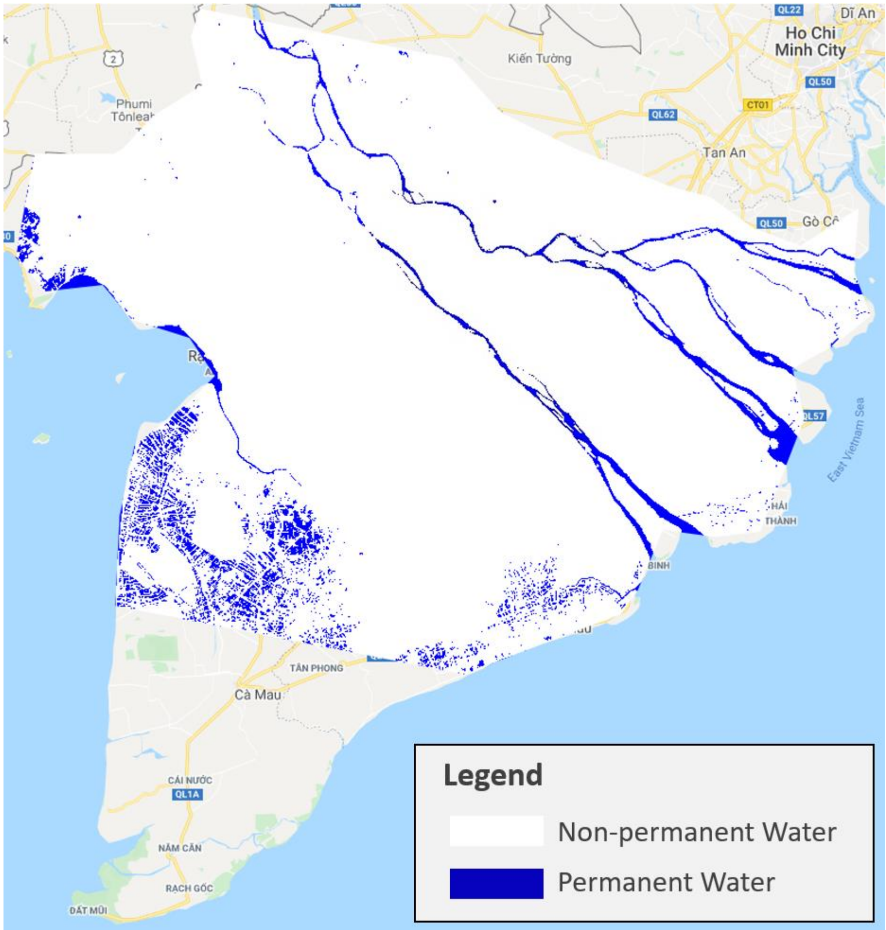

Figure 7. Permanent Water Map from 2016 to 2020

4.2.2. Trends of Surface Water

The water surface is extracted from the data of five years, and the trends of the inundated pixels can be shown and summarized. In other words, this line chart also shows the trend of the total surface water area over the past five years. We can see clear periods of dry and flood seasons. The flood period is from September to December, and the drought period is from January to August every year. According to news and flood reports, the flood period in the Mekong Delta is getting increasingly dry after 2018, which is also reflected in this trend figure.

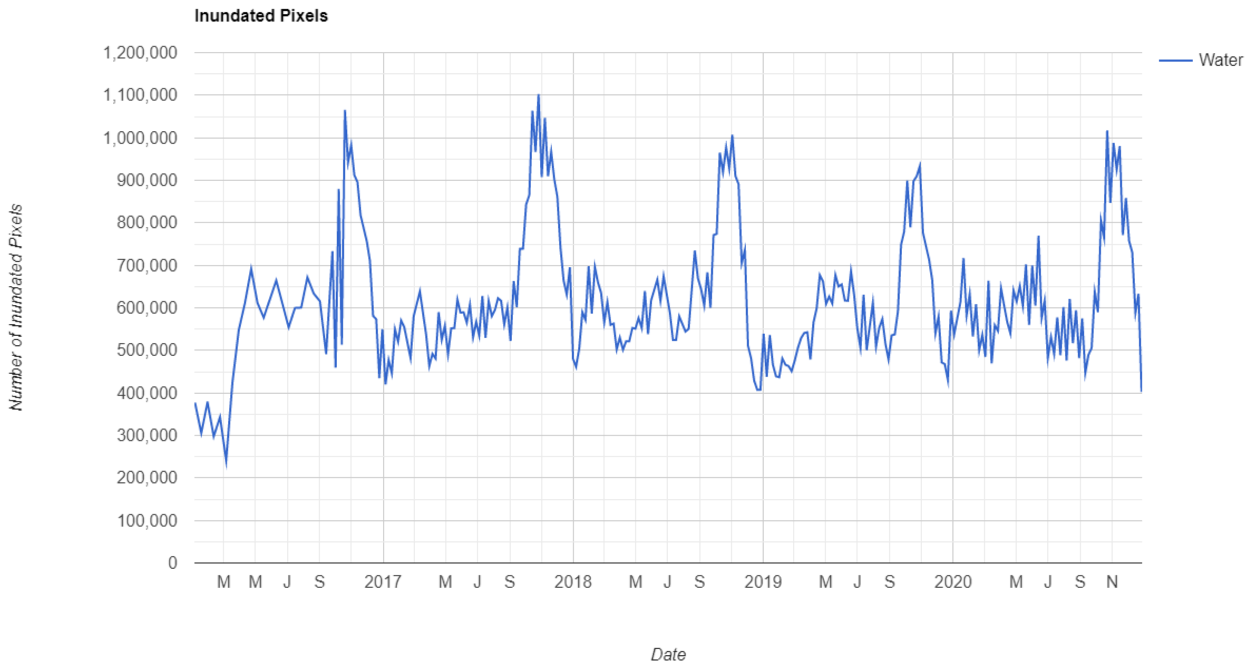

Figure 8. Trend of Total Surface Water from 2016 to 2020

When the permanent water surface is calculated and masked off, we can also get the trend chart of seasonal water surface, shown as follows.

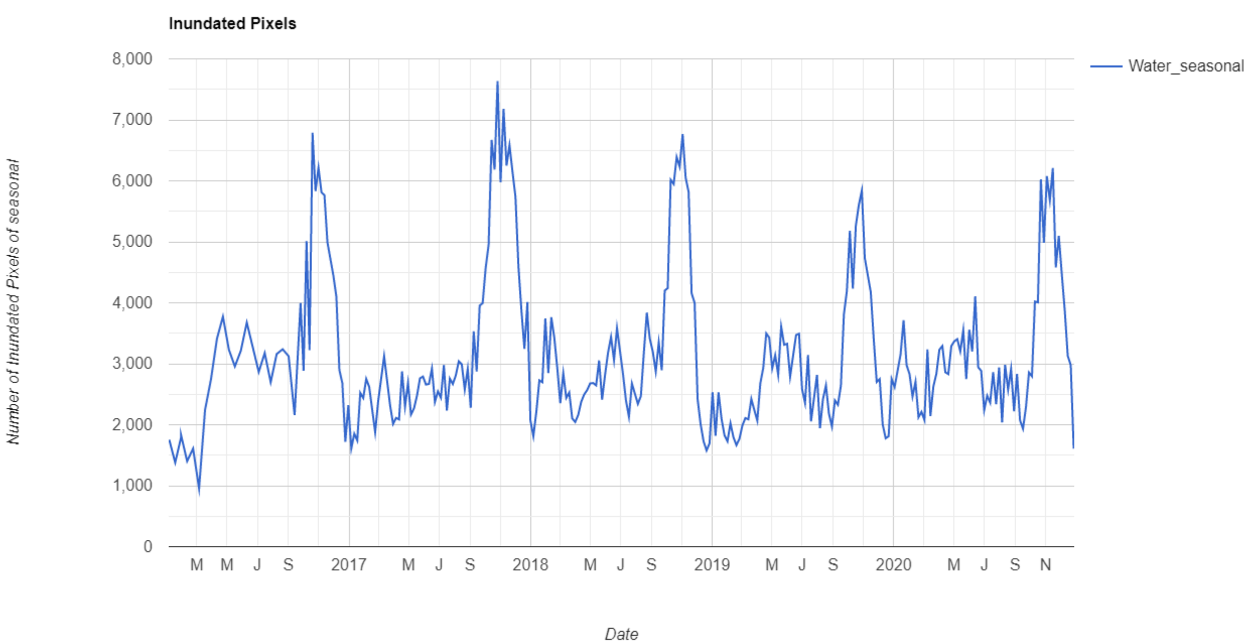

Figure 9. Trend of Seasonal Surface Water from 2016 to 2020

Theoretically, the trend of seasonal water surface is closer to the real trend of flood conditions, comparing with the total water surface. However, in addition to the difference in numbers of inundated pixels, the overall trend and information of seasonal water surface are similar to the total water surface. This also shows that the permanent water surface in this delta area has been relatively stable in the past five years.

4.3. Damage Assessment of Annual Maximum Flood Events

4.3.1. Annual Maximum Events

The annual maximum flood events can be selected in the previous trend maps. All five annual maximum flood events, and their information of periods before and during the flood are summarized in the following table.

Table 6. Annual Maximum Events Selection from 2016 to 2020

Year	Annual Maximum Event	Period Before Event	Period During Event
2016	2016/10/19	10/11 - 10/17	10/18 - 10/24
2017	2017/10/26	9/22 – 9/28	10/22 – 10/28
2018	2018/11/02	9/21 – 9/27	10/29 – 11/04
2019	2019/10/28	9/19 – 9/25	10/25 – 10/31
2020	2020/10/22	10/05 – 10/11	10/20 – 10/26

It can be seen that the most serious floods occur from mid-October to early November every year. Sometimes floods occur continuously, resulting in a large number of inundated pixels for a long time. In order to obtain more comparable information, the period before event is always set to be within the end of the dry season in the year. In this way, we can compare the difference between the end of drought period and the period during the extreme flood, so as to conduct the damage analysis.

4.3.2. Affected Area

The difference layer can be obtained for each flood event. Area with blue indicates the inundated pixels. Also, the flood area can be computed, shown in the table.

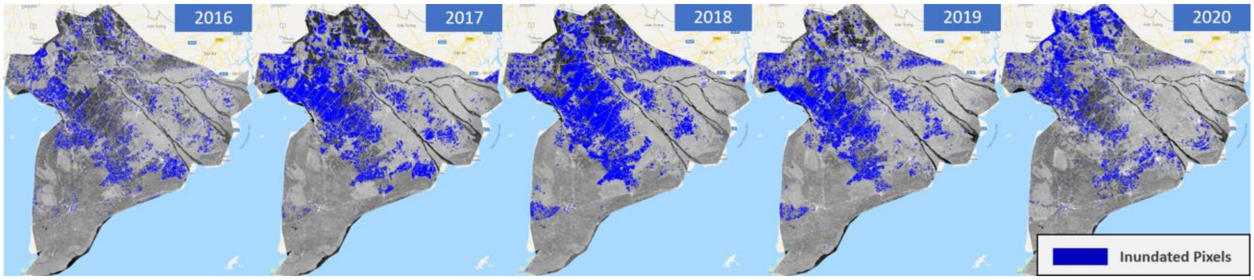

Figure 10. The Inundated Pixels in Extreme Events from 2016 to 2020

Table 7. Affected Area in Extreme Events from 2016 to 2020

Year	2016	2017	2018	2019	2020
Affected Area (Hectares)	545,423	662,546	695,117	606,159	504,835

The trend of the affected area through 2016 to 2020 can be visualized in the following line chart.

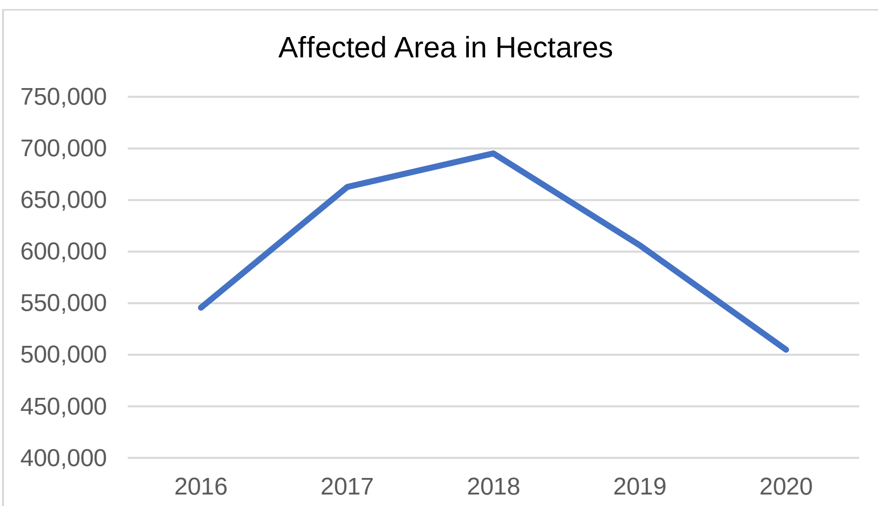

Figure 11. The Affected Area Trend in Extreme Events from 2016 to 2020

In the past five years, the area affected by extreme flood events was over 500,000 hectares every year. Compared the data within these five years, the affected area is the largest in 2018, which is nearly 700,000 hectares. Since then, the impact of extreme flood events has been relatively reduced every year.

4.3.3. Exposed Population

The exposed population can also be shown after the difference layer intersecting with the Global Human Settlement Layer. The scattered area in red indicates higher population that has affected by extreme event.

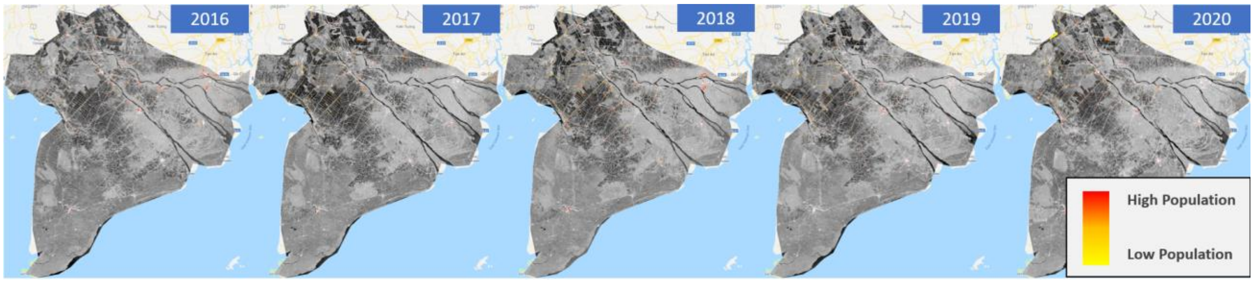

Figure 12. The Exposed Population in Extreme Events from 2016 to 2020

Table 8. Exposed Population in Extreme Events from 2016 to 2020

Year	2016	2017	2018	2019	2020
Exposed Population	1,332,680	1,009,051	1,500,517	1,170,149	1,159,200

The trend of the affected population through 2016 to 2020 can be visualized in the following line chart.

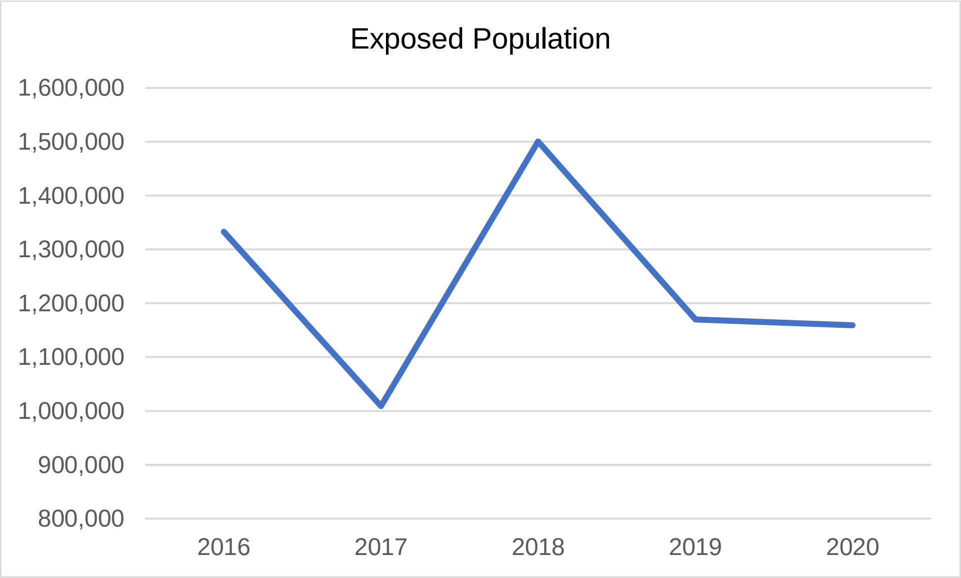

Figure 13. The Exposed Population Trend in Extreme Events from 2016 to 2020

Except for 2018, the population exposed to extreme events has stabilized at around 1 - 1.2 million. The extreme flood events in 2018 have a particularly great impact on the overall area and exposed population.

CHAPTER 5: Conclusion

This paper mainly studied the surface water extraction methods based on Sentinel Data, and evaluated the accuracy of different methods, so as to select the most accurate and workable method to extract the water surface through 2016 to 2020. Then, under the timeline, the permanent water and non-permanent water can be classified using threshold in frequency. Also, the pixel-based trends of total water surface and seasonal (non-permanent) water surface can be displayed using line charts. Furthermore, when we look at the annual extreme flood events through 2016 to 2020, the simple damage assessment maps can be obtained to show the affected flood area and exposed population. Through these processes and discussion, we can acquire some basic understanding of the flood situation in Mekong Delta in recent years. It also helps to be more familiar with the operations of processing and analyzing of remote sensing data under the timeline based on GEE platform.

However, on the whole, this study has many limitations that cannot be ignored. First, because sentinel data is only available in the earliest year of 2014, the trend analysis does not contain much information of a long-time dimension. Secondly, theoretically, using Sentinel-2 multispectral data to extract water surface enables higher accuracy, but this study lacks more accurate methods to remove cloud effects, which makes the method of extracting water surface relatively ineffective. Moreover, for further analysis, the damage assessment of extreme flood events can include more aspects, such as the affected cropland or urban area, displaced homes and so on.

In conclusion, this study records my exploration of the flooding situation in Mekong Delta, and also of the Sentinel data and GEE platform. It is the first step for me to conduct the study in the field of remote sensing, and I hope to continue and improve the results in the future.

REFERENCE

Andreassen, L. M., Melvold, K., Müller, K., Nagy, T., Orthe, N. K., & Winsvold, S. H. (n.d.). *Using the Sentinels to detect glacier lake outburst floods, snow avalanches and the glacier, lake ice and snow cover in Norway*. 1.

Arias, M. (2013). *Impacts of Hydrological Alterations in the Mekong Basin to the Tonle Sap Ecosystem*.

Boateng, I. (2012). GIS assessment of coastal vulnerability to climate change and coastal adaption planning in Vietnam. *Journal of Coastal Conservation*, *16*(1), 25–36. https://doi.org/10.1007/s11852-011-0165-0

Brisco, B., Touzi, R., Sanden, J. J. van der, Charbonneau, F., Pultz, T. J., & D'Iorio, M. (2008). Water resource applications with RADARSAT-2 – a preview. *International Journal of Digital Earth*, *1*(1), 130–147. https://doi.org/10.1080/17538940701782577

Brown, A. R., Petropoulos, G. P., & Ferentinos, K. P. (2018). Appraisal of the Sentinel-1 & 2 use in a large-scale wildfire assessment: A case study from Portugal's fires of 2017. *Applied Geography*, *100*, 78–89. https://doi.org/10.1016/j.apgeog.2018.10.004

Chandrasekar, K., Sesha Sai, M. V. R., Roy, P. S., & Dwevedi, R. S. (2010). Land Surface Water Index (LSWI) response to rainfall and NDVI using the MODIS Vegetation Index product. *International Journal of Remote Sensing*, *31*(15), 3987–4005. https://doi.org/10.1080/01431160802575653

Commission (MRC), M. R. (n.d.-a). *Flood and Drought*. Retrieved May 25, 2021, from https://www.mrcmekong.org/our-work/topics/flood-and-drought/

Commission (MRC), M. R. (n.d.-b). *Geography*. Retrieved May 25, 2021, from https://www.mrcmekong.org/about/mekong-basin/geography/

Cvar, A. (2013). *GIS-based reservoir planning with limited data in developing nations: A case study of the Lower Mekong River Basin* [Text, Colorado State University]. https://mountainscholar.org/handle/10217/88421

Danaher, T., & Collett, L. (2006). Development, optimisation and multi-temporal application of a simple Landsat based water index. *Proceeding of the 13th Australasian Remote Sensing and Photogrammetry Conference, Canberra, ACT, Australia*, *2024*.

Das, N. N., Entekhabi, D., Dunbar, R. S., Chaubell, M. J., Colliander, A., Yueh, S., Jagdhuber, T., Chen, F., Crow, W., O'Neill, P. E., Walker, J. P., Berg, A., Bosch, D. D., Caldwell, T., Cosh, M. H., Collins, C. H., Lopez-Baeza, E., & Thibeault, M. (2019). The SMAP and Copernicus Sentinel 1A/B microwave active-passive high resolution surface soil moisture product. *Remote Sensing of Environment*, *233*, 111380. https://doi.org/10.1016/j.rse.2019.111380

Dinh, Q., Balica, S., Popescu, I., & Jonoski, A. (2012). Climate change impact on flood hazard, vulnerability and risk of the Long Xuyen Quadrangle in the Mekong Delta. *International Journal of River Basin Management*, *10*(1), 103–120. https://doi.org/10.1080/15715124.2012.663383

Divergent trends of open-surface water body area in the contiguous United States from 1984 to 2016 | PNAS. (n.d.). Retrieved May 25, 2021, from https://www.pnas.org/content/115/15/3810

Drusch, M., Del Bello, U., Carlier, S., Colin, O., Fernandez, V., Gascon, F., Hoersch, B., Isola, C., Laberinti, P., Martimort, P., Meygret, A., Spoto, F., Sy, O., Marchese, F., & Bargellini, P. (2012). Sentinel-2: ESA's Optical High-Resolution Mission for GMES Operational Services. *Remote Sensing of Environment*, *120*, 25–36. https://doi.org/10.1016/j.rse.2011.11.026

El Hajj, M., Baghdadi, N., Zribi, M., & Bazzi, H. (2017). Synergic Use of Sentinel-1 and Sentinel-2 Images for Operational Soil Moisture Mapping at High Spatial Resolution over Agricultural Areas. *Remote Sensing*, *9*(12), 1292. https://doi.org/10.3390/rs9121292

Feyisa, G. L., Meilby, H., Fensholt, R., & Proud, S. R. (2014). Automated Water Extraction Index: A new technique for surface water mapping using Landsat imagery. *Remote Sensing of Environment*, *140*, 23–35. https://doi.org/10.1016/j.rse.2013.08.029

Fisher, A., Flood, N., & Danaher, T. (2016). Comparing Landsat water index methods for automated water classification in eastern Australia. *Remote Sensing of Environment*, *175*, 167–182. https://doi.org/10.1016/j.rse.2015.12.055

Gálya, B., Blaskó, L., Nagy, A., Juhász, C., Riczu, P., & Tamás, J. (2018). *Spatial segmentation of inland water surface using C-band synthetic aperture radar images on the Great Hungarian Plain*. *20*, 13618.

Global Human Settlement—GHS BUILT-UP GRID - European Commission. (n.d.). Retrieved May 25, 2021, from https://ghsl.jrc.ec.europa.eu/ghs_bu.php

Greifeneder, F., Wagner, W., Sabel, D., & Naeimi, V. (2014). Suitability of SAR imagery for automatic flood mapping in the Lower Mekong Basin. *International Journal of Remote Sensing*, *35*(8), 2857–2874. https://doi.org/10.1080/01431161.2014.890299

Hoang-Phi, P., Lam-Dao, N., Pham-Van, C., Chau-Nguyen-Xuan, Q., Nguyen-Van-Anh, V., Gummadi, S., & Le-Van, T. (2020). Sentinel-1 SAR Time Series-Based Assessment of the Impact of Severe Salinity Intrusion Events on Spatiotemporal Changes in Distribution of Rice Planting Areas in Coastal Provinces of the Mekong Delta, Vietnam. *Remote Sensing*, *12*(19), 3196. https://doi.org/10.3390/rs12193196

Kenduiywo, B. K., Bargiel, D., & Soergel, U. (2018). Crop-type mapping from a sequence of Sentinel 1 images. *International Journal of Remote Sensing*, *39*(19), 6383–6404. https://doi.org/10.1080/01431161.2018.1460503

Kuenzer, C., Klein, I., Ullmann, T., Georgiou, E., Baumhauer, R., & Dech, S. (2015). Remote Sensing of River Delta Inundation: Exploiting the Potential of Coarse Spatial Resolution, Temporally-Dense MODIS Time Series. *Remote Sensing*, *7*(7), 8516–8542. https://doi.org/10.3390/rs70708516

Leinenkugel, P., Wolters, M. L., Oppelt, N., & Kuenzer, C. (2015). Tree cover and forest cover dynamics in the Mekong Basin from 2001 to 2011. *Remote Sensing of Environment*, *158*, 376–392. https://doi.org/10.1016/j.rse.2014.10.021

Liu, S., Lu, P., Liu, D., Jin, P., & Wang, W. (2009). Pinpointing the sources and measuring the lengths of the principal rivers of the world. *International Journal of Digital Earth*, *2*(1), 80–87. https://doi.org/10.1080/17538940902746082

McFEETERS, S. K. (1996). The use of the Normalized Difference Water Index (NDWI) in the delineation of open water features. *International Journal of Remote Sensing*, *17*(7), 1425–1432. https://doi.org/10.1080/01431169608948714

Mekong a "treasure trove" of 1,000 newly discovered species—CNN.com. (n.d.). Retrieved May 25, 2021, from http://www.cnn.com/2008/TECH/science/12/16/rat.mekong/index.html

MEKONG FLOODS ARE A REMINDER OF A PERENNIAL RISK. (n.d.). Retrieved May 25, 2021, from https://www.jbarisk.com/flood-services/event-response/mekong-delta-flood-report/

Mirelva, P. R., & Nagasawa, R. (2019). Application of Sentinel-1 Data for Classifying Croplands Using Google Earth Engine. *International Journal of Geoinformatics*, *15*(3), 21–31.

Missions—Sentinel Online—Sentinel. (n.d.). Retrieved May 25, 2021, from https://sentinel.esa.int/web/sentinel/missions

Nigussie, W., Hailu, B. T., & Azagegn, T. (2019). Mapping of groundwater potential zones using sentinel satellites (−1 SAR and -2A MSI) images and analytical hierarchy process in Ketar watershed, Main Ethiopian Rift. *Journal of African Earth Sciences*, *160*, 103632. https://doi.org/10.1016/j.jafrearsci.2019.103632

Pekel, J.-F., Cottam, A., Gorelick, N., & Belward, A. S. (2016). High-resolution mapping of global surface water and its long-term changes. *Nature*, *540*(7633), 418–422. https://doi.org/10.1038/nature20584

Pham-Duc, B., Prigent, C., & Aires, F. (2017). Surface Water Monitoring within Cambodia and the Vietnamese Mekong Delta over a Year, with Sentinel-1 SAR Observations. *Water*, *9*(6), 366. https://doi.org/10.3390/w9060366

Poenaru, V., Moise, C., Negula, I. D., Badea, A., Vladucu, A., Stanisteanu, L., & Mainerici, M. (2018). *Detection of irrigated crops from Sentinel 1 and Sentinel 2 data to estimate seasonal water use. A case study: Banat pilot area, Romania*. *20*, 19282.

Reducer Overview | Google Earth Engine. (n.d.). Google Developers. Retrieved May 26, 2021, from https://developers.google.com/earth-engine/guides/reducers_intro

Report: Flooded Future: Global vulnerability to sea level rise worse than previously understood. (n.d.). Retrieved May 25, 2021, from https://www.climatecentral.org/news/report-flooded-future-global-vulnerability-to-sea-level-rise-worse-than-previously-understood

Sakamoto, T., Van Nguyen, N., Kotera, A., Ohno, H., Ishitsuka, N., & Yokozawa, M. (2007). Detecting temporal changes in the extent of annual flooding within the Cambodia and the Vietnamese Mekong Delta from MODIS time-series imagery. *Remote Sensing of Environment*, *109*(3), 295–313. https://doi.org/10.1016/j.rse.2007.01.011

Sentinel-1 SAR GRD: C-band Synthetic Aperture Radar Ground Range Detected, log scaling. (n.d.). Retrieved May 25, 2021, from https://developers.google.com/earth-engine/datasets/catalog/COPERNICUS_S1_GRD

Sentinel-2 MSI: MultiSpectral Instrument, Level-2A. (n.d.). Google Developers. Retrieved May 25, 2021, from https://developers.google.com/earth-engine/datasets/catalog/COPERNICUS_S2_SR

Shao, Y., & Wang, L. (2020). GEE 云平台支持下的西天山森林遥感监测与时空变化分析 [Remote sensing monitoring and spatial-temporal change analysis of forest in western Tianshan mountains supported by GEE cloud platform]. *Bulletin of Surveying and Mapping*. Retrieved May 25, 2021, from https://kns.cnki.net/kcms/detail/detail.aspx?doi=10.13474/j.cnki.11-2246.2020.0240

SNAP – STEP. (n.d.). Retrieved May 25, 2021, from https://step.esa.int/main/toolboxes/snap/

Sneddon, C., & Fox, C. (2006). Rethinking transboundary waters: A critical hydropolitics of the Mekong basin. *Political Geography*, *25*(2), 181–202. https://doi.org/10.1016/j.polgeo.2005.11.002

Step-by-Step: Recommended Practice: Flood Mapping and Damage Assessment using Sentinel-1 SAR data in Google Earth Engine. (n.d.). UN-SPIDER Knowledge Portal. Retrieved May 25, 2021, from https://www.un-spider.org/advisory-support/recommended-practices/recommended-practice-google-earth-engine-flood-mapping/step-by-step

VietnamPlus. (2019, October 4). *Urban areas in Mekong Delta face serious flooding | Environment | Vietnam+ (VietnamPlus)*. VietnamPlus. https://en.vietnamplus.vn/urban-areas-in-mekong-delta-face-serious-flooding/161556.vnp

Wang, D., Wang, S., & Huang, C. (2019). Sentinel-2 和 Landsat 8 影像的四种常用水体指数地表水体提取对比 [Comparison of Sentinel-2 imagery with Landsat 8 imagery for surface water extraction using four common water indices]. *Remote Sensing for Land and Resources.* Retrieved May 26, 2021, from http://www.gtzyyg.com/article/2019/1001-070X/1001-070X-31-3-157.shtml

Wassmann, R., Hien, N. X., Hoanh, C. T., & Tuong, T. P. (2004). Sea Level Rise Affecting the Vietnamese Mekong Delta: Water Elevation in the Flood Season and Implications for Rice Production. *Climatic Change*, *66*(1), 89–107. https://doi.org/10.1023/B:CLIM.0000043144.69736.b7

Wassmann, R., Phong, N. D., Tho, T. Q., Hoanh, C. T., Khoi, N. H., Hien, N. X., Vo, T. B. T., & Tuong, T. P. (2019). High-resolution mapping of flood and salinity risks for rice production in the Vietnamese Mekong Delta. *Field Crops Research*, *236*, 111–120. https://doi.org/10.1016/j.fcr.2019.03.007

Wayand, N. E., Marsh, C. B., Shea, J. M., & Pomeroy, J. W. (2018). Globally scalable alpine snow metrics. *Remote Sensing of Environment*, *213*, 61–72. https://doi.org/10.1016/j.rse.2018.05.012
Weichselgartner, J. (2004). *From the Field: Flood Disaster Mitigation in the Mekong Delta*.
Xia, H., Zhao, J., Qin, Y., Yang, J., Cui, Y., Song, H., Ma, L., Jin, N., & Meng, Q. (2019). Changes in Water Surface Area during 1989–2017 in the Huai River Basin using Landsat Data and Google Earth Engine. *Remote Sensing*, *11*(15), 1824. https://doi.org/10.3390/rs11151824
Xu, H. (2005). A study on information extraction of water body with the modified normalized difference water index (MNDWI). *Journal of Remote Sensing*, *9*, 589–595.
Zhou, H., Ye, H., Wei, X., Zhang, Z., Wang, F., Qi, Y., & Ma, J. (2019). 基于 Sentinel-1/2 的水体提取方法对比研究——以斯里兰卡小型水体为例 [Comparative study on water extraction methods based on Sentinel-1/2: a case study of small water body in Sri Lanka]. *Journal of University of Chinese Academy of Sciences.* Retrieved May 25, 2021, from http://html.rhhz.net/ZGKXYDXXB/20190610.htm